Available online at www.sciencedirect.com
SCIENCE DIRECT®
Spectrochimica Acta Part A 61 (2005) 515–525
SPECTROCHIMICA ACTA PART A
www.elsevier.com/locate/saa

Infrared spectroscopy of organoclays synthesized with the surfactant octadecyltrimethylammonium bromide

Yunfei Xi [a], Zhe Ding [a], Hongping He [b], Ray L. Frost [a,*]

[a] *Inorganic Materials Research Group, School of Physical and Chemical Sciences, Queensland University of Technology, G.P.O. Box 2434, Brisbane, Qld 4001, Australia*
[b] *Guangzhou Institute of Geochemistry, Chinese Academy of Sciences, Wushan, Guangzhou 510640, China*

Received 30 March 2004; accepted 3 May 2004

Abstract

Infrared (IR) spectroscopy using a smart endurance single bounce diamond attenuated total reflection (ATR) cell has been used to study the changes in the spectra of the surfactant octadecyltrimethylammonium (ODTMA) bromide upon intercalation into a sodium montmorillonite. The wavenumbers of bands attributed to CH-stretching and CH-bending vibrations, in general, decrease as the concentration of the surfactant measured in terms of the cation exchange capacity (CEC) up to 1.0 CEC. After this point, the bands increase approaching a value the same as that of the surfactant. Significant changes occur in the HCH deformation modes of the methyl groups of the surfactant. These changes are attributed to the methyl groups locking into the siloxane (SiO) surface of the montmorillonite. Such a concept is supported by changes in the SiO-stretching bands of the montmorillonite siloxane surface.

Keywords: Infrared spectroscopy; Octadecyltrimethylammonium bromide; Montmorillonite; Surfactant

1. Introduction

Organoclays may be synthesised by ion exchange of the mono or divalent cation Na^+, Mg^{2+} or Ca^{2+} with a large organic cation, such as octadecyltrimethylammonium (ODTMA) bromide. The properties of these materials change from hydrophilic to hydrophobic/lipophilic. These clays may then have useful properties, for example, the removal of oil, toxic chemicals and humic materials from water [1–3]. These modified minerals, organoclays, represent a family of materials which have a lot of applications in a range of key areas, such as adsorbents for organic pollutants [4,5], rheological control agents [6], reinforcing fillers for plastics and electric materials [7–9].

The influence of montmorillonite surfaces on the chemical and physical properties of adsorbed H_2O molecules has been the subject of a number of recent studies using structural, thermodynamic, spectroscopic and computational methods. Generally, the position of the ν_2 mode of H_2O decreases and H_2O-sretching band shifts to higher wavenumber upon lowering the H_2O content in cation exchanged montmorillonite. At the same time, the cation type is determinative for total water content retained in clay minerals. However, to the best of our knowledge, there is no report about the sorbed H_2O molecules in organoclays and it is very important for the application of organoclays. Hence, the situation of the sorbed H_2O molecules in organoclays at different surfactant concentrations is discussed in this paper. Recently, FTIR spectroscopy using attenuated total reflection (ATR) and KBr pressed disk techniques has been used to characterize sorbed water and $HDTMA^+$ in organoclay [10]. It was found that sorbed water content decreases with the intercalation of $HDTMA^+$. In this work we extend these studies to the changes in the surfactant upon intercalation. Attenuated total reflection technique has been used to study the changes in structure of the organoclay formed between a montmorillonitic clay and octadecyltrimethylammonium bromide.

2. Experimental

2.1. Materials

The montmorillonite used in this study was supplied by the Clay Minerals Society as source clay SWy-2-Na-

* Corresponding author. Tel.: +61 7 3864 2407; fax: +61 7 3864 1804.
E-mail address: r.frost@qut.edu.au (R.L. Frost).

1386-1425/$ – see front matter © 2004 Elsevier B.V. All rights reserved.
doi:10.1016/j.saa.2004.05.001

Table 1
Table of the infrared bands for octadecyltrimethylammonium bromide and octadecyltrimethylammonium bromide-intercalated montmorillonite

	CEC	0	0.2	0.4	0.6	0.8	1.0	1.5	2.0	3.0	4.0	ODTMA
1	Center	3627	3628	3629	3630	3629	3630	3629	3629	3629	3629	*
	FWHM	65.2	62.5	60.9	61.0	61.7	63.4	61.3	61.3	60.8	60.5	*
	%Area	1.23	2.80	1.08	0.96	0.87	0.93	0.91	1.00	0.85	0.83	*
2	Center	3573	3566	3560	3549	3532	3530	3519	3519	3533	3526	*
	FWHM	137.8	133.3	140.0	151.7	177.3	126.3	175.4	165.5	148.7	161.2	*
	%Area	0.61	1.05	0.72	0.59	0.48	0.46	0.29	0.47	0.25	0.32	*
3	Center	3414	3410	3410	3404	3391	3420	3397	3388	3386	3382	3372
	FWHM	238.9	234.7	236.8	226.4	235.0	203.1	226.9	187.1	209.9	203.3	218.8
	%Area	5.20	8.22	4.09	2.92	2.54	1.79	2.60	2.64	2.86	2.77	1.85
4	Center	3221	3223	3227	3224	3215	3243	3226	3228	3203	3206	*
	FWHM	181.6	189.6	185.9	185.6	159.6	219.9	227.3	212.0	158.2	0.37	*
	%Area	1.99	3.66	2.28	1.84	0.73	1.16	1.08	0.97	0.40	3034	*
5	Center	3076	3094	3118	3121	3080	3054	3054	3050	3036	93.9	3041
	FWHM	176.5	216.1	177.1	109.2	128.4	158.7	37.7	53.8	80.1		123.3
	%Area	0.39	0.81	0.52	0.18	0.23	0.18	0.03	0.10	0.24	0.32	0.96
6	Center	*	*	*	*	*	3050	3035	3029	3031	3031	3031
	FWHM	*	*	*	*	*	31.2	23.4	22.6	9.5	9.3	7.4
	%Area	*	*	*	*	*	0.01	0.02	0.04	0.02	0.03	0.22
7	Center	*	*	*	3049	3041	3030	3023	3017	3018	3017	3017
	FWHM	*	*	*	49.6	43.8	15.0	14.4	16.1	10.8	9.8	8.4
	%Area	*	*	*	0.04	0.02	0.00	0.01	0.03	0.05	0.06	0.56
8	Center	*	*	*	*	*	3021	3015	3003	3008	3008	3008
	FWHM	*	*	*	*	*	5.7	9.5	10.4	11.7	11.8	11.0
	%Area	*	*	*	*	*	0.00	0.00	0.00	0.01	0.02	0.36
9	Center	*	2958	2958	2960	2954	2953	2961	2956	2959	2959	2959
	FWHM	*	9.2	12.4	9.1	3.5	12.0	17.0	13.7	4.9	4.5	6.8
	%Area	*	0.00	0.01	0.00	0.00	0.00	0.02	0.03	0.01	0.01	0.31
10	Center	*	2946	2943	2942	2943	2945	2944	2941	2946	2946	2950
	FWHM	*	39.6	40.9	41.0	43.9	46.6	38.0	46.6	39.7	40.0	9.3
	%Area	*	0.15	0.24	0.32	0.47	0.62	0.59	0.79	0.83	0.84	1.33
11	Center	2939	2936	2936	2938	2940	2941	2936	2935	2936	2941	2943
	FWHM	80.4	10.5	11.9	10.0	11.8	12.4	10.9	13.5	29.0	21.9	7.2
	%Area	0.06	0.02	0.04	0.03	0.05	0.08	0.07	0.10	0.15	0.17	0.51
12	Center	*	2929	2928	2931	2932	2933	2929	2928	2928	2928	2936
	FWHM	*	14.5	14.5	10.7	11.5	11.8	11.3	11.4	12.5	11.6	18.3
	%Area	*	0.05	0.08	0.09	0.11	0.17	0.21	0.26	0.26	0.24	0.34
13	Center	*	2927	2926	2926	2926	2926	2922	2920	2921	2921	2922
	FWHM	*	13.8	13.0	12.9	13.7	12.1	13.1	10.6	10.2	9.7	8.5
	%Area	*	0.07	0.10	0.15	0.18	0.24	0.51	0.42	0.36	0.37	0.52
14	Center	*	2922	2921	2922	2921	2920	2916	2915	2915	2915	2916
	FWHM	*	25.1	25.7	19.9	18.2	16.1	11.9	11.8	12.5	12.5	13.7
	%Area	*	0.23	0.32	0.34	0.30	0.42	0.74	1.40	2.34	2.78	24.17
15	Center	*	2906	2902	2904	2903	2902	2902	2903	2899	2898	2896
	FWHM	*	66.2	98.6	85.8	62.0	57.1	67.9	65.9	46.3	46.0	34.9
	%Area	*	0.25	1.04	1.28	1.10	1.49	2.60	2.83	2.14	2.63	11.79
16	Center	*	2874	2874	2873	2874	2874	2872	2872	2871	2871	2871
	FWHM	*	6.0	6.9	12.4	17.6	17.0	15.0	9.8	7.9	7.0	6.1
	%Area	*	0.00	0.00	0.01	0.06	0.08	0.07	0.04	0.04	0.04	0.33
17	Center	*	2855	2855	2853	2851	2851	2850	2849	2849	2849	2852
	FWHM	*	15.3	16.3	20.2	21.5	23.5	12.7	11.0	10.5	10.4	7.2
	%Area	*	0.21	0.27	0.50	0.72	1.12	0.97	1.40	1.82	2.32	0.81

Table 1 (*Continued*)

	CEC	0	0.2	0.4	0.6	0.8	1.0	1.5	2.0	3.0	4.0	ODTMA
18	Center	*	2845	2847	2843	2840	2840	2845	2847	2848	2848	2848
	FWHM	*	18.6	20.0	21.1	18.9	20.3	25.8	27.0	24.6	26.6	8.8
	%Area	*	0.07	0.14	0.22	0.29	0.34	0.58	0.57	0.76	0.63	14.14
19	Center	1672	*	*	*	*	*	*	*	*	*	*
	FWHM	64.1	*	*	*	*	*	*	*	*	*	*
	%Area	0.25	*	*	*	*	*	*	*	*	*	*
20	Center	1647	1636	1635	1637	1641	1643	1644	1644	1643	1642	*
	FWHM	39.1	57.2	54.2	49.9	44.1	39.5	47.4	54.0	57.7	57.7	*
	%Area	0.20	1.92	1.07	0.79	0.56	0.42	0.46	0.52	0.50	0.50	*
21	Center	1628	*	*	*	*	*	*	*	*	*	1623
	FWHM		*	*	*	*	*	*	*	*	*	20.0
	%Area		*	*	*	*	*	*	*	*	*	0.03
22	Center	*	1492	1490	1491	1492	1493	1493	1495	1495	1495	1489
	FWHM	*	8.0	9.2	9.1	9.7	9.3	12.3	14.1	11.9	11.6	1.9
	%Area	*	0.02	0.04	0.05	0.05	0.06	0.08	0.12	0.10	0.10	0.09
23	Center	*	1488	1487	1488	1488	1488	1488	1487	1487	1487	1487
	FWHM	*	6.1	6.2	6.5	6.7	7.0	9.6	11.8	9.2	8.2	5.6
	%Area	*	0.03	0.04	0.06	0.08	0.10	0.19	0.30	0.41	0.46	2.68
24	Center	*	1480	1479	1479	1479	1481	1481	1479	1480	1480	1480
	FWHM	*	13.2	17.2	15.3	14.9	13.7	11.3	8.5	6.4	5.9	6.5
	%Area	*	0.01	0.03	0.05	0.06	0.08	0.07	0.12	0.10	0.12	1.57
25	Center	*	1476	1476	1476	1475	1475	1474	1472	1472	1472	1473
	FWHM	*	7.5	8.7	11.7	13.2	13.8	13.9	10.6	8.8	8.5	5.6
	%Area	*	0.03	0.05	0.13	0.16	0.22	0.36	0.37	0.58	0.62	3.28
26	Center	*	1472	1473	1472	1471	1470	1470	1469	1467	1467	1464
	FWHM	*	14.1	14.2	13.8	13.4	14.5	7.2	9.4	5.9	6.7	3.8
	%Area	*	0.06	0.11	0.10	0.14	0.20	0.08	0.09	0.11	0.18	0.05
27	Center	*	1468	1468	1467	1467	1467	1466	1466	1463	1463	1462
	FWHM	*	6.8	8.9	8.7	7.9	8.9	9.0	9.5	7.2	7.0	6.0
	%Area	*	0.01	0.03	0.06	0.07	0.09	0.22	0.29	0.23	0.31	4.13
28	Center	*	1465	1462	1460	1459	1459	1458	1457	1457	1456	1444
	FWHM	*	29.4	18.9	23.1	23.2	24.7	19.5	17.3	26.4	33.6	27.2
	%Area	*	0.11	0.10	0.18	0.18	0.19	0.23	0.23	0.30	0.34	0.86
29	Center	1439	1436	1440	1437	1437	1436	1438	1440	1433	1431	1431
	FWHM	75.4	23.2	25.2	22.5	21.6	19.2	21.2	23.4	18.9	12.2	7.6
	%Area	0.08	0.03	0.06	0.06	0.07	0.05	0.08	0.12	0.09	0.08	0.88
30	Center	*	1417	1417	1417	1417	1417	1417	1418	1418	1418	*
	FWHM	*	8.3	9.7	11.1	11.5	10.1	11.2	11.0	9.1	9.5	*
	%Area	*	0.02	0.03	0.05	0.06	0.05	0.07	0.07	0.05	0.05	*
31	Center	*	1410	1398	1401	1399	1401	1400	1407	1408	1408	1408
	FWHM	*	28.7	14.8	14.9	16.8	17.5	11.9	9.8	8.3	7.6	6.6
	%Area	*	0.02	0.01	0.01	0.02	0.01	0.01	0.01	0.04	0.06	0.88
32	Center	*	1390	1390	1390	1389	1390	1392	1395	1396	1396	1396
	FWHM	*	12.4	8.2	9.5	10.2	10.7	10.4	13.1	8.7	8.2	8.5
	%Area	*	0.00	0.00	0.01	0.01	0.01	0.01	0.03	0.03	0.04	0.60
33	Center	*	1381	1380	1379	1377	1377	1377	1377	1379	1380	1382
	FWHM	*	27.4	17.2	22.2	20.1	20.6	26.0	18.7	25.3	24.0	7.3
	%Area	*	0.02	0.02	0.04	0.04	0.06	0.09	0.07	0.12	0.13	0.68
34	Center	1152	1158	1158	1159	1159	1159	1159	1159	1161	1162	*
	FWHM	60.8	60.3	63.0	62.1	61.5	61.2	57.5	53.1	53.9	46.8	*
	%Area	2.03	1.41	1.62	1.41	1.30	1.19	1.13	1.04	0.97	0.81	*

Table 1 (*Continued*)

	CEC	0	0.2	0.4	0.6	0.8	1.0	1.5	2.0	3.0	4.0	ODTMA
35	Center	1133	1141	1138	1140	1140	1143	1142	1136	1139	1140	*
	FWHM	28.2	17.0	23.6	21.3	21.4	18.2	14.3	22.1	18.7	18.9	*
	%Area	0.65	0.11	0.28	0.18	0.18	0.13	0.06	0.39	0.14	0.18	*
36	Center	1116	1122	1122	1122	1120	1117	1116	1117	1118	1118	*
	FWHM	24.4	27.4	22.3	25.2	25.2	29.6	30.6	21.7	26.1	27.6	*
	%Area	1.04	1.22	0.88	1.00	0.99	1.05	1.17	1.16	1.14	1.28	*
37	Center	1094	1111	1110	1110	1109	1110	1108	1097	1103	1104	*
	FWHM	34.4	34.1	36.5	35.6	35.7	36.2	36.7	33.9	36.8	36.7	*
	%Area	1.65	1.82	2.49	2.32	2.22	1.72	1.85	2.34	2.28	2.36	*
38	Center	1064	1087	1085	1084	1083	1083	1082	1077	1080	1080	*
	FWHM	15.8	26.3	25.0	24.9	24.3	26.4	24.9	20.0	23.9	24.4	*
	%Area	0.19	1.13	1.17	1.12	0.81	1.01	1.02	0.63	1.04	1.15	*
39	Center	1031	1037	1040	1040	1040	1036	1037	1037	1039	1040	*
	FWHM	57.7	50.1	47.8	46.1	42.3	42.7	40.5	40.2	40.8	41.2	*
	%Area	14.88	14.40	14.21	14.00	13.13	12.46	12.79	13.27	13.51	14.75	*
40	Center	989	998	1000	1000	1000	996	998	999	1002	1003	*
	FWHM	52.9	51.0	52.3	52.0	51.6	48.9	48.5	46.6	47.2	48.7	*
	%Area	21.79	21.32	26.59	29.83	36.11	37.82	38.05	39.14	34.59	33.90	*
41	Center	972	969	970	969	966	965	965	966	965	965	966
	FWHM	41.4	42.5	41.3	41.6	39.3	32.0	31.3	28.8	27.0	25.9	10.2
	%Area	7.14	8.15	8.10	8.27	7.57	3.15	2.86	2.64	5.23	5.59	3.13
42	Center	952	954	955	954	952	951	951	951	949	949	949
	FWHM	29.6	32.5	32.1	30.9	29.8	28.8	29.7	27.4	24.2	17.6	8.7
	%Area	3.50	3.86	4.02	3.70	3.25	2.40	2.10	2.09	2.69	1.62	1.92
43	Center	937	940	942	942	943	935	934	939	923	923	932
	FWHM	28.7	23.1	23.8	23.4	18.4	24.5	28.5	17.4	5.9	6.1	7.7
	%Area	1.43	0.83	0.86	0.73	0.13	0.58	0.43	0.22	0.04	0.06	0.11
44	Center	921	922	923	922	923	921	921	920	921	920	924
	FWHM	55.9	52.7	52.8	51.4	51.5	50.8	50.9	48.5	54.9	60.2	4.6
	%Area	14.16	10.29	11.52	10.83	10.51	10.95	9.72	4.97	8.36	9.17	0.34
45	Center	910	912	912	912	912	911	910	909	910	910	911
	FWHM	28.8	26.3	25.4	24.4	22.4	22.3	21.6	21.9	17.9	14.3	10.2
	%Area	3.79	2.40	2.25	2.10	1.86	2.13	2.05	2.56	2.04	1.39	6.39
46	Center	875	880	881	881	882	882	882	882	883	883	891
	FWHM	36.2	31.9	31.3	31.6	30.5	31.4	31.4	31.8	32.2	32.3	7.7
	%Area	7.28	5.66	5.94	6.16	5.63	6.88	6.18	6.18	5.06	2.38	0.45
47	Center	847	845	844	845	856	856	858	857	857	857	857
	FWHM	20.1	24.3	44.9	24.7	13.7	20.3	15.4	18.9	14.7	12.4	6.1
	%Area	0.62	0.25	2.56	0.10	0.06	0.24	0.12	0.23	0.17	0.16	0.32
48	Center	838	844	844	844	843	842	843	842	843	843	826
	FWHM	50.1	44.7	20.2	39.6	31.8	34.3	32.8	32.0	31.6	31.0	5.6
	%Area	3.05	2.24	0.15	2.20	1.55	2.01	1.71	1.51	1.15	1.05	0.15
49	Center	797	797	797	797	798	798	798	798	798	798	801
	FWHM	19.7	19.7	19.2	20.0	20.5	21.2	20.4	19.6	18.4	17.7	6.1
	%Area	2.23	1.09	1.16	1.23	1.16	1.40	1.21	1.17	0.93	1.71	0.19
50	Center	789	788	788	788	788	789	788	788	789	789	796
	FWHM	13.3	12.7	12.5	14.3	15.8	14.2	14.9	15.4	14.8	15.2	4.6
	%Area	0.34	0.23	0.25	0.28	0.32	0.38	0.37	0.45	0.42	0.46	0.08
51	Center	777	778	778	777	778	777	777	777	777	777	776
	FWHM	14.9	13.7	13.1	12.5	12.1	12.3	12.0	12.2	11.9	11.5	5.3
	%Area	0.98	0.68	0.67	0.61	0.51	0.65	0.55	0.60	0.49	0.46	0.08
52	Center	765	766	768	767	767	766	766	767	766	766	761
	FWHM	24.5	24.8	25.1	25.8	22.8	20.9	21.5	20.4	20.3	19.5	4.5
	%Area	0.78	0.57	0.53	0.49	0.32	0.45	0.42	0.41	0.32	0.30	0.11

Table 1 (*Continued*)

	CEC	0	0.2	0.4	0.6	0.8	1.0	1.5	2.0	3.0	4.0	ODTMA
53	Center	748	751	750	750	756	753	755	754	754	754	754
	FWHM	22.8	24.3	25.8	25.2	11.4	16.7	9.1	10.5	5.4	5.3	5.1
	%Area	0.33	0.21	0.17	0.11	0.01	0.02	0.01	0.04	0.02	0.02	0.24
54	Center	726	728	733	730	729	730	730	728	730	730	731
	FWHM	23.9	28.6	23.0	23.0	17.5	17.8	17.4	18.5	10.3	8.7	5.6
	%Area	0.56	0.79	0.35	0.34	0.27	0.45	0.45	0.58	0.41	0.42	2.20
55	Center	712	714	720	722	723	722	720	720	719	719	719
	FWHM	12.4	12.9	23.8	25.7	24.5	19.0	13.2	10.5	9.0	8.4	5.5
	%Area	0.07	0.06	0.39	0.44	0.46	0.53	0.51	0.53	0.69	0.78	1.88
56	Center	696	694	694	694	694	695	695	695	695	695	*
	FWHM	26.5	27.3	21.6	21.9	19.3	20.7	21.1	19.3	19.9	20.2	*
	%Area	0.60	0.60	0.42	0.41	0.29	0.35	0.33	0.30	0.26	0.28	*
57	Center	618	623	622	623	622	622	623	623	623	624	*
	FWHM	14.1	14.1	17.1	16.6	17.8	18.2	18.5	19.4	19.1	18.1	*
	%Area	0.19	0.28	0.54	0.60	0.93	0.91	1.03	1.41	1.26	1.27	*
58	Center	604	608	607	608	606	607	607	605	607	608	*
	FWHM	16.3	22.8	24.3	25.6	21.4	25.1	28.2	29.2	29.7	28.8	*
	%Area	0.19	0.53	0.35	0.46	0.76	0.53	0.63	0.71	0.73	0.72	*

Montmorillonite (Wyoming). This clay originates from the Newcastle formation, (cretaceous), County of Crook, State of Wyoming, USA. The cation exchange capacity (CEC) is 76.4 meq per 100 g (according to the specification of its producer). The surfactant used in this study is octadecyltrimethylammonium bromide ($C_{21}H_{46}NBr$, FW: 392.52) from Sigma-Aldrich.

2.2. Preparation

The syntheses of surfactant–clay hybrids were undertaken by the following procedure: 4 g of SWy-2-Na-montmorillonite was first dispersed in 400 ml of deionized water and then stirred with a Heidolph magnetic stirrer at about 600 rpm for about 16 h. A pre-dissolved stoichiometric amount of octadecyltrimethylammonium bromide solution was slowly added to the clay suspension at 60 °C.

The concentrations of $ODTMA^+$ used are 0.2 CEC, 0.4 CEC, 0.6 CEC, 0.8 CEC, 1.0 CEC, 1.5 CEC, 2.0 CEC, 3.0 CEC and 4.0 CEC of the SWy-2-montmorillonite, respectively. The reaction mixtures were stirred for 30 min at 60 °C using a Branson Ultrasonics model 250 sonifier with an output of 40 mW. All organoclay products were washed of bromide anions, dried at room temperature and then ground in an agate mortar, stored in a vacuum desiccator for about 7 days.

2.3. Infrared spectroscopy

Infrared (IR) spectra were obtained using a Nicolet Nexus 870 FTIR spectrometer with a smart endurance single bounce diamond ATR cell. Spectra over the 4000–525 cm^{-1}

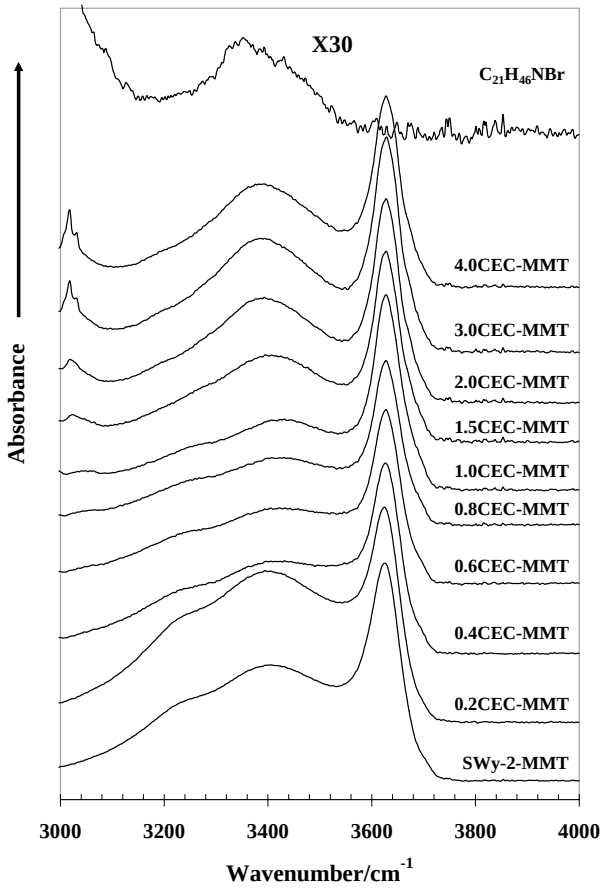

Fig. 1. Infrared spectra of montmorillonite, cation exchanged montmorillonite over the concentration range 0.2–4.0 CEC and octadecyltrimethylammonium bromide in the 3000–4000 cm^{-1} spectral range.

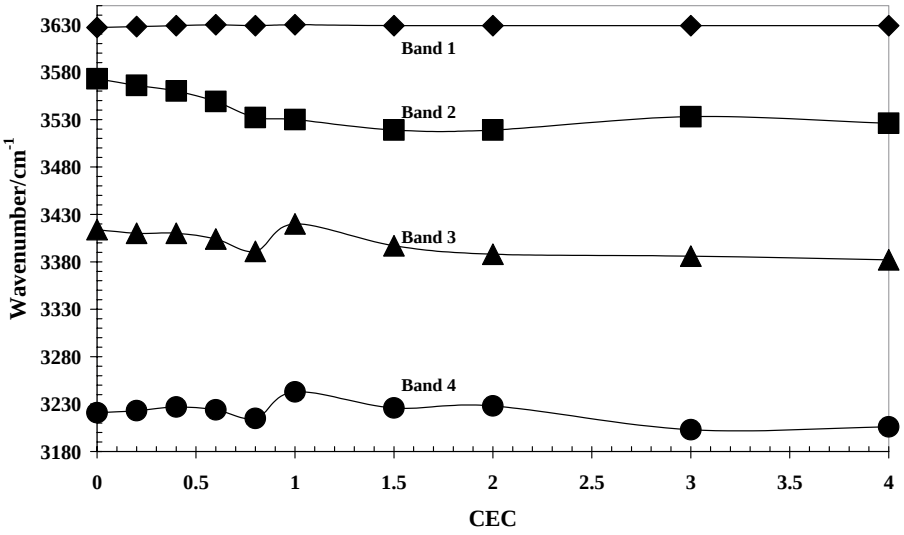

Fig. 2. Variation in wavenumber for the bands 1–4 observed at 3627, 3573, 3414 and 3221 cm^{-1}.

range were obtained by the co-addition of 64 scans with a resolution of 4 cm^{-1} and a mirror velocity of 0.6329 cm s^{-1}. Spectral manipulation such as baseline adjustment, smoothing and normalisation was performed using the GRAMS® software package (Galactic Industries Corporation, Salem, NH, USA).

3. Results and discussion

3.1. OH and NH stretching region

The infrared spectroscopy of the montmorillonitic clay modified with octadecyltrimethylammonium bromide (OMMT) may be divided into sections according to the functional groups. For example the hydroxyl (OH)-stretching region and the CH-stretching region. The hydroxyl-stretching region is shown in Fig. 1. The results of the band component analyses are reported in Table 1. Table 1 lists the bands in terms of a number from the highest wavenumber to the lowest wavenumber. The figure shows that there are no bands in this region resulting from octadecyltrimethylammonium bromide. An intense relatively sharp band is observed at 3629 cm^{-1}, with an average bandwidth of around 61.3 cm^{-1}. The band is unaffected by the presence of the octadecyltrimethylammonium bromide and is assigned to the OH-stretching vibration of the montmorillonitic clay (Fig. 2). The spectral profile in the 3000–3550 cm^{-1} region changes significantly with the concentration of surfactant molecules. Bands in this region are ascribed to adsorbed water. A band is observed at 3573 cm^{-1} the position of which is dependent upon the concentration of the surfactant

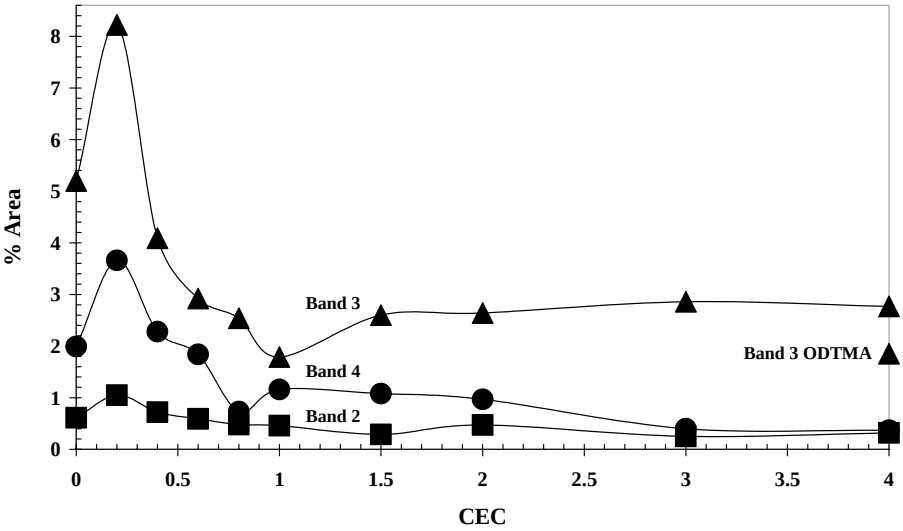

Fig. 3. Variation in intensity for the bands 2–4 observed at 3573, 3414 and 3221 cm^{-1}.

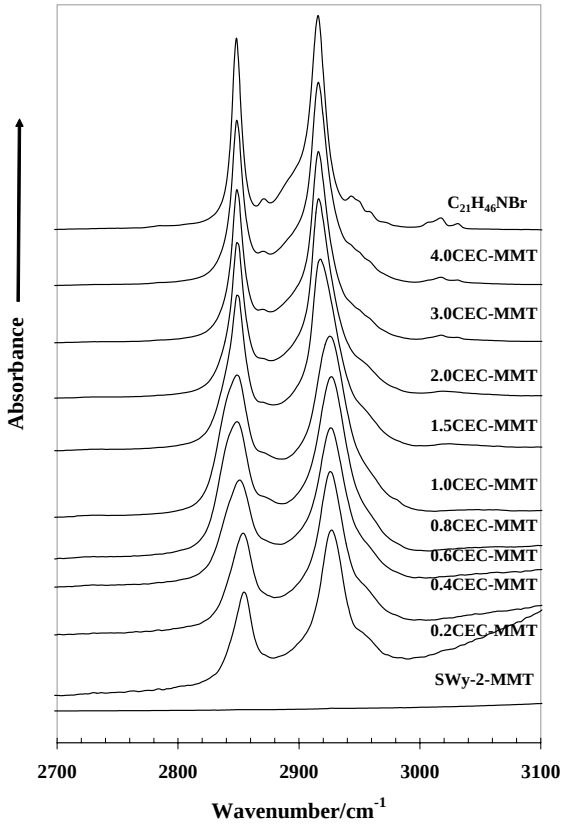

Fig. 4. Infrared spectra of montmorillonite, cation exchanged montmorillonite over the concentration range 0.2–4.0 CEC and octadecyltrimethylammonium bromide in the 2700–3100 cm^{-1} spectral range.

intercalated into the montmorillonite as is shown in Fig. 2. The intensity of this band decreases with surfactant concentration and is attributed to water hydrating the cation in the montmorillonite interlayer. Two bands are observed at 3414 and 3221 $cm^{-1,}$ the wavenumber of which decreases, jumps at 1 CEC and then decreases. These bands may be initially attributed to water-stretching modes. At 0.6 CEC, the spectral profile changes and a band at around 3400 cm^{-1} appears to increase in intensity (Fig. 3). This band is assigned to the OH-stretching vibration of adsorbed water. The change in wavenumber is related to the environment of the water. Up to 1.0 CEC, the water is in the montmorillonite interlayer and is gradually displaced by the octadecyltrimethylammonium bromide as the concentration increases. Above 1.0 CEC, the surfactant is adsorbed on other octadecyltrimethylammonium bromide molecules already in the clay interlayer.

3.2. CH-stretching vibrations

The spectra of the CH-stretching region for the MMT and OMMT at various CEC concentrations and the pure surfactant are shown in Fig. 4. The spectrum of the octadecyltrimethylammonium bromide shows bands at 3041, 3031, 3017, 3008, 2959, 2950, 2943, 2936, 2922, 2916, 2896, 2871, 2852 and 2848 cm^{-1}. The variation in wavenumber for bands 11–14 is shown in Fig. 5. The band at 2936 cm^{-1} (band 11) increases in wavenumber up to the 1.0 CEC; then decreases in wavenumber. A similar effect is observed for band 12 at 2929 cm^{-1}. The wavenumber then increases towards the value for the surfactant. These two bands are attributed to CH-stretching modes of the methyl groups of the octadecyltrimethylammonium bromide. The increase in wavenumber with CEC is ascribed to the locking in of the methyl groups into the siloxane layer. The two bands at 2922 and 2906 cm^{-1} are attributed to CH vibrations of the octadecyl part of the surfactant molecule. The wavenumber of these bands decreases with increase of surfactant concentration. The variation in intensity of these bands is shown in Fig. 6.

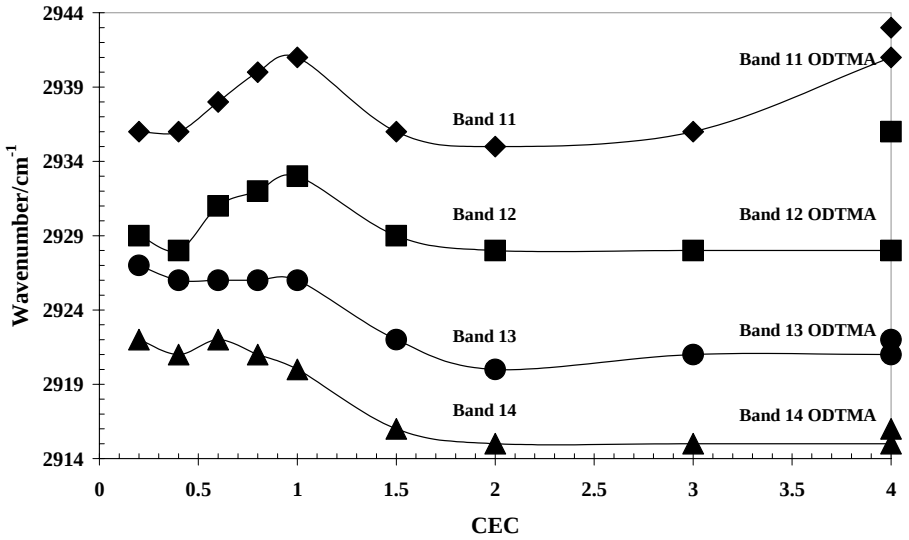

Fig. 5. Variation in wavenumber for the bands 11–14 observed at 2943, 2936, 2922, 2916 and 2896 cm^{-1}.

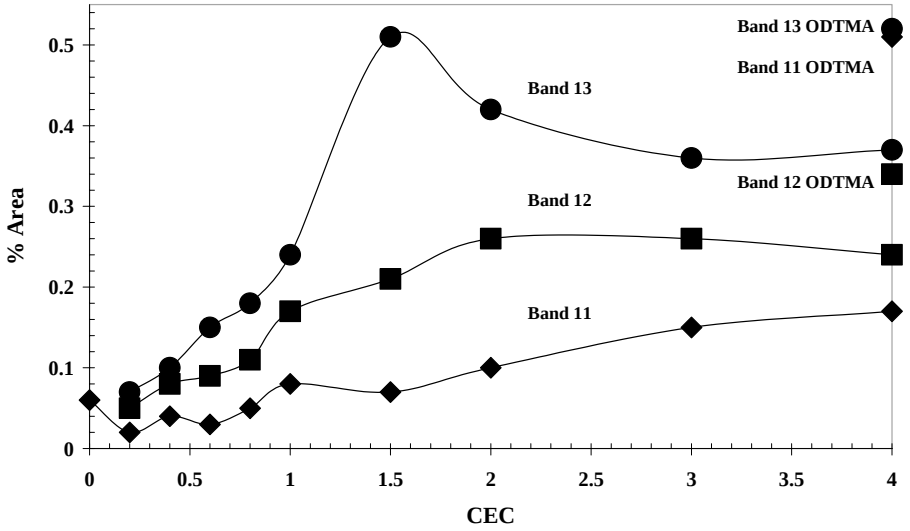

Fig. 6. Variation in intensity for the bands 11–14 observed at 2943, 2936, 2922, 2916 and 2896 cm^{-1}.

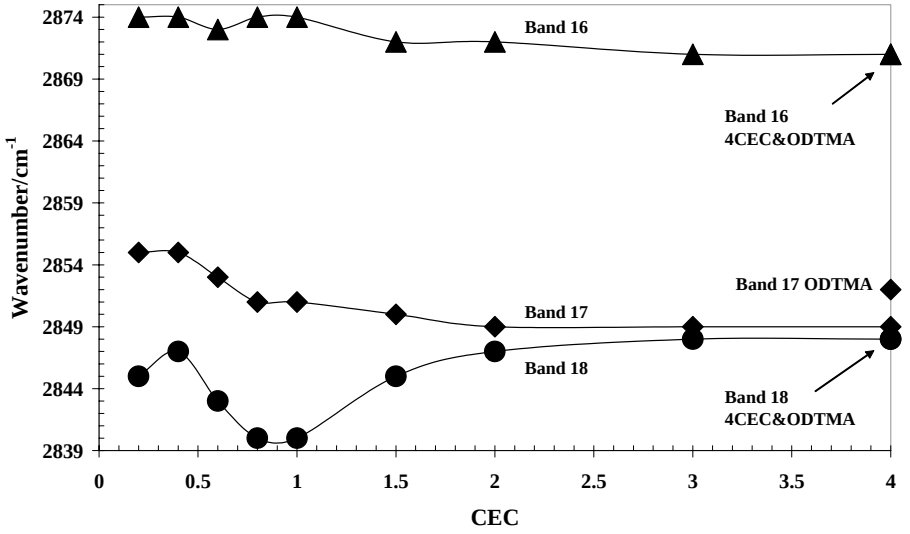

Fig. 7. Variation in wavenumber for the bands 16–18 observed at 2943, 2936, 2922, 2916 and 2896 cm^{-1}.

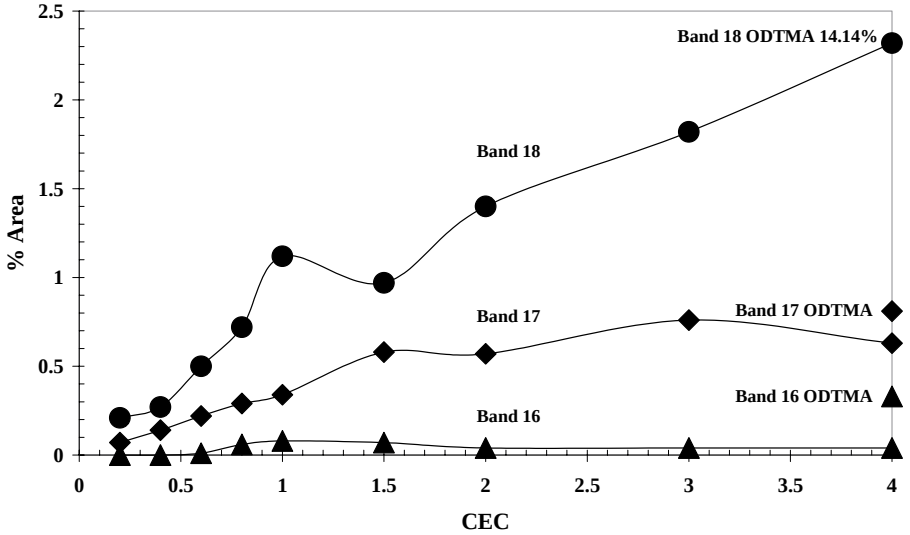

Fig. 8. Variation in intensity for the bands 16–18 observed at 2943, 2936, 2922, 2916 and 2896 cm^{-1}.

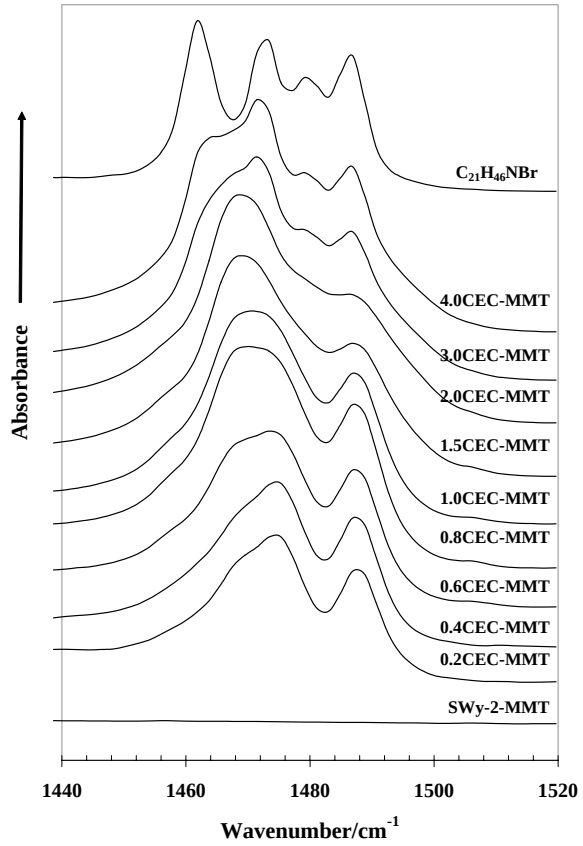

Fig. 9. Infrared spectra of montmorillonite, cation exchanged montmorillonite over the concentration range 0.2–4.0 CEC and octadecyltrimethylammonium bromide in the 1440–1520 cm^{-1} spectral range.

The variation in the wavenumber for bands 16, 17 and 18 are shown in Fig. 7. The position of band 16 shows a slight decrease in wavenumber as the CEC concentration of surfactant is increased. Bands 17 and 18 show a more pronounced change in band position with increasing CEC. There is an initial increase in wavenumber followed by a decrease up to 1.0 CEC followed by an increase. The intensity of these bands at 2874, 2855 and 2845 cm^{-1} increases with increase in CEC concentration (Fig. 8). The intensity of the bands approaches the intensity of the non-intercalated surfactant.

Previous study proposed that both the frequencies of antisymmetric and symmetric CH_2-stretching modes of amine chains are extremely sensitive to the conformational changes of the chains and their wavenumbers will decrease as the increase of ordered conformers within clay interlayers, and only when the chains are highly ordered (all-trans conformation), the narrow absorption bands appear around 2916 ($\nu_{as}(CH_2)$) and 2848 cm^{-1} (ν_s (CH_2)) in the infrared spectrum [11]. However, our present study indicates that only the wavenumber of antisymmetric CH_2-stretching mode is sensitive to the conformational change of amines within the clay interlayer. This is similar to our previous study on $HDTMA^+$ in organoclay [10] and provides another evidence for our previous proposal that the antisymmetric CH_2-stretching mode is more sensitive to the conformational ordering than the symmetric stretching mode does.

3.3. HCH bending vibrations

The HCH deformation region of the octadecyltrimethylammonium bromide intercalated montmorillonite is shown in Fig. 9. This region is a window in which no bands from the clay are found. Specific conclusions can be made from the spectra in Fig. 9. The spectrum of unreacted octadecyltrimethylammonium bromide is very different from the octadecyltrimethylammonium bromide in the montmorillonite interlayer. Major bands in the 1440–1520 cm^{-1}

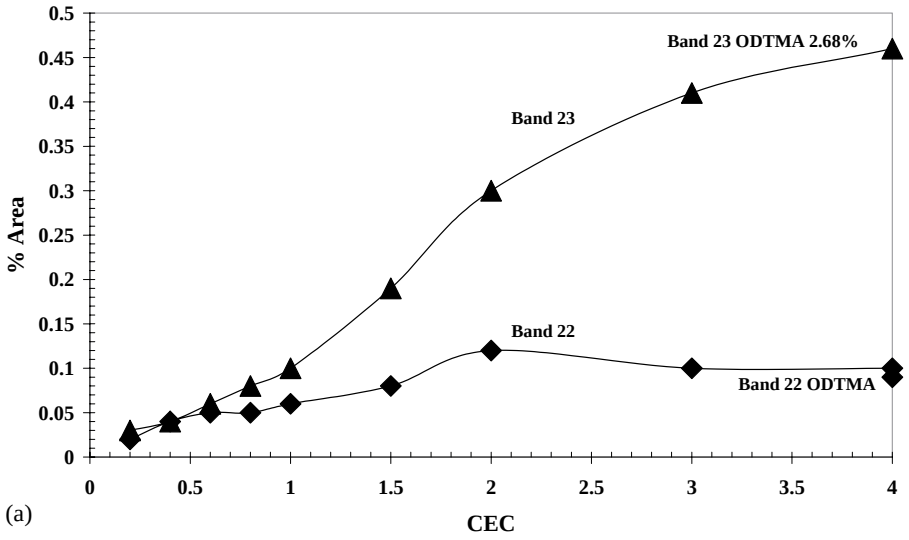

Fig. 10. (a) Variation in intensity for the bands 22 and 23 observed at 1492 and 1488 cm^{-1}. (b) Variation in intensity for the bands 22 and 23 observed at 1480 and 1473 cm^{-1}.

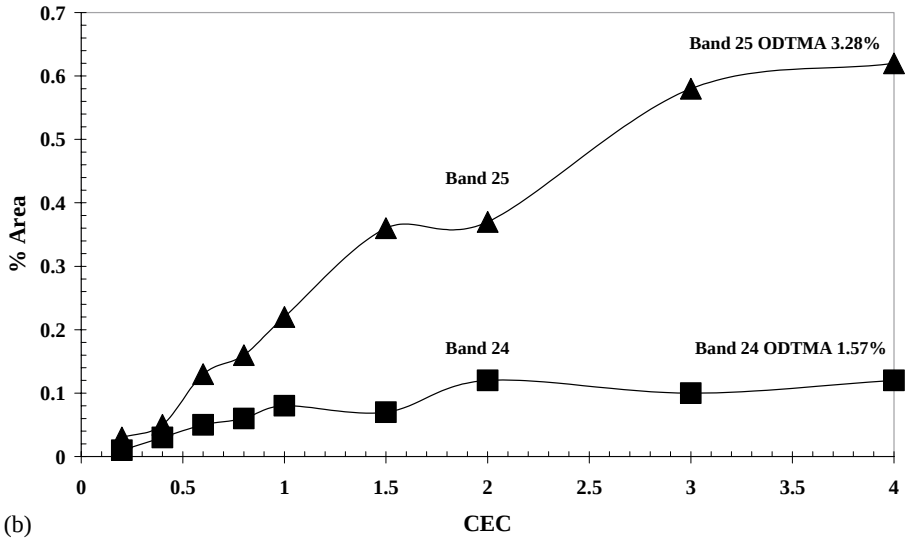

Fig. 10. (*Continued*).

spectral region are found for the surfactant at 1489, 1487, 1480, 1473, 1464, 1462 and 1444 cm^{-1}. The band at 1464 cm^{-1} is not observed in the low CEC surfactant modified montmorillonite. Only after the 1.0 CEC mark is significant intensity observed. The band at 1480 cm^{-1} is also not observed until after the 3.0 CEC concentration. These results show significant changes in the methyl deformation region. The methyl groups are probably linked into the siloxane surface [12]; and hence the free rotation of the methyl groups is lost. The variation in intensity of these bands is shown in Fig. 10a and b. The low wavenumber region of the surfactant modified clay is shown in Fig. 11. The bands in this region are predominantly attributed to the montmorillonite. Four bands are observed at 966, 949, 932 and 911 cm^{-1} and are attributed to the octadecyltrimethylammonium bromide. Two bands are observed at 730 and 719 cm^{-1} and are attributed to the surfactant.

Bands in the 989 to 1152 cm^{-1} region are attributed to SiO-stretching vibrations. These bands are observed at 1152, 1133, 1116, 1094, 1064, 1031 and 989 cm^{-1}. No bands are observed in these positions for the octadecyltrimethylammonium bromide. The 1152 cm^{-1} band shifts incrementally to 1162 cm^{-1} at the 4.0 CEC. This is a shift of 10 cm^{-1}. As the change in wavenumbers occurs, there is a decrease in the relative intensity of the band as the concentration of the surfactant increases. The band at 1133 cm^{-1} shifts to 1140 cm^{-1} and the band at 1094 cm^{-1} shifts to 1104 cm^{-1}. The infrared bands, observed at 1064 and 1031 cm^{-1}, for the untreated montmorillonite show a shift in band position upon immediate contact with the octadecyltrimethylammonium bromide surfactant. The significance of these results rests with the interaction between the octadecyltrimethylammonium bromide molecules and the siloxane surface. These results mean that there is an interaction between the surfactant molecule and the montmorillonite siloxane layer immediately upon contact. As the CEC increases, the bands shift to higher wavenumbers. This is proposed as an increase in interaction/bonding between the surfactant molecules and the siloxane surface.

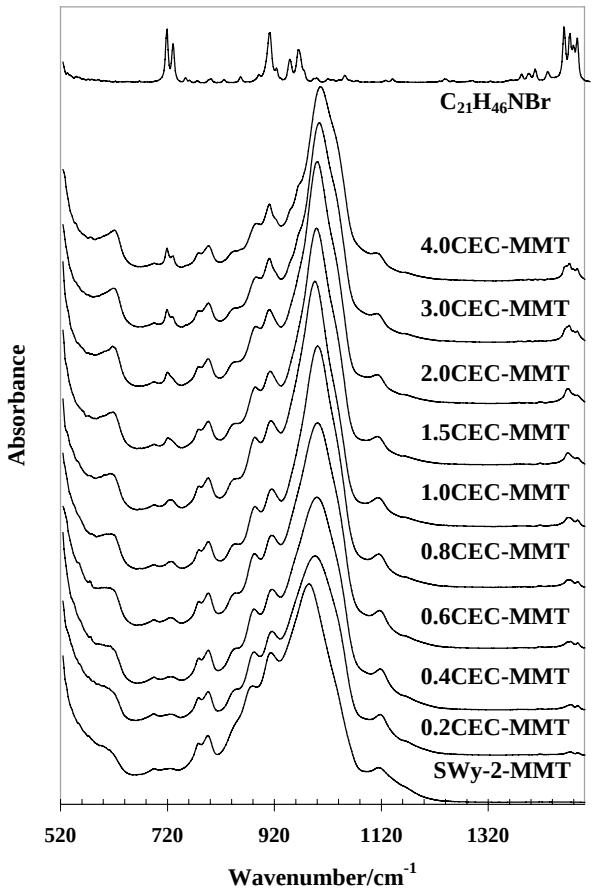

Fig. 11. Infrared spectra of montmorillonite, cation exchanged montmorillonite over the concentration range 0.2–4.0 CEC and octadecyltrimethylammonium bromide in the 520–1400 cm^{-1} spectral range.

4. Conclusions

Infrared ATR techniques have been used to study the changes in the wavenumbers of octadecyltrimethylammonium bromide upon intercalation into montmorillonite. The spectra of the ODTMA-intercalated montmorillonite are very different from the pure octadecyltrimethylammonium bromide. Changes in both the wavenumber and the intensity of the bands occur as the CEC increases. In general, there is a decrease in wavenumber with increasing CEC concentration up to 1.0 CEC; after this point the wavenumber increases up to 4.0 CEC the value at which is close to the value for the pure octadecyltrimethylammonium bromide. Bands which are attributed to water-stretching vibrations decrease in intensity as the ion exchange of the sodium from the montmorillonite occurs. After 1.0 CEC, no intensity remains in these water bands.

Marked changes occur in the surface properties of montmorillonitic clay when the cation Na^+ is replaced with an organocation, in this case; octadecyltrimethylammonium bromide. The clay changes from being hydrophilic to hydrophobic and becomes lipophilic.

Acknowledgements

The financial and infra-structure support of the Queensland University of Technology, Inorganic Materials Research Program of the School of Physical and Chemical Sciences is gratefully acknowledged. The Australian Research Council (ARC) is being thanked for funding. The Queensland Main Roads Department is being thanked for funding the scholarship of Y. Xi.

References

[1] L. Zhu, Q. Pan, S. Chen, J. Zhang, L. Wei, Shuichuli Jishu 22 (1996) 107.
[2] H. Zhao, G.F. Vance, Water Res. 32 (1998) 3710.
[3] S. Yariv, Thermochim. Acta 274 (1996) 1.
[4] R.S. Taylor, M.E. Davies, J. Williams, in: PCT Int. Appl., Laporte Industries Ltd., UK, Wo, 1992, p. 16.
[5] X. Wang, S. Wu, W. Li, G. Sheng, Huanjing Huaxue 16 (1997) 1.
[6] P.A. Sutton, in: Proceedings of the 78th Annual Meeting Technical Program of the FSCT, 2000, p. 637.
[7] I.D. Sand, R.L. Piner, J.W. Gilmer, J.T. Owens, in: U.S., Eastman Chemical Company, USA, 2003, p. 8.
[8] M. Rafailovich, M. Si, M. Goldman, in: PCT Int. Appl. (The Research Foundation of State University of New York, USA), Wo, 2003, p. 34.
[9] T.J. Pinnavaia, T. Lan, Z. Wang, H. Shi, P.D. Kaviratna, ACS Symp. Ser. 622 (1996) 250.
[10] H. He, R.L. Frost, Y. Xi, J. Zhu, J. Raman Spectrosc. 35 (2004) 316.
[11] Y. Li, H. Ishida, Langmuir 19 (2003) 2479.
[12] A. Vahedi-Faridi, S. Guggenheim, Clays Clay Miner. 45 (1997) 859.